Electrolyte-Gated Transistors Based on Conducting Polymer Nanowire Junction Arrays

Maksudul M. Alam, Jun Wang, Yaoyao Guo, Stephanie P. Lee, and Hsian-Rong Tseng*

Crump Institute for Molecular Imaging, Department of Molecular and Medical Pharmacology, David Geffen School of Medicine, University of California, 700 Westwood Plaza, Los Angeles, California 90095

Received: February 21, 2005; In Final Form: April 15, 2005

In this study, we describe the electrolyte gating and doping effects of transistors based on conducting polymer nanowire electrode junction arrays in buffered aqueous media. Conducting polymer nanowires including polyaniline, polypyrrole, and poly(ethylenedioxythiophene) were investigated. In the presence of a positive gate bias, the device exhibits a large on/off current ratio of 978 for polyaniline nanowire-based transistors; these values vary according to the acidity of the gate medium. We attribute these efficient electrolyte gating and doping effects to the electrochemically fabricated nanostructures of conducting polymer nanowires. This study demonstrates that two-terminal devices can be easily converted into three-terminal transistors by simply immersing the device into an electrolyte solution along with a gate electrode. Here, the field-induced modulation can be applied for signal amplification to enhance the device performance.

Introduction

Conducting polymer nanowires[1−6] are promising one-dimensional nanostructured materials for applications in nanoelectronic devices[4,7] and in chemo-[2,8] and biosensors[9] because of their light weights, large surface areas, adjustable transport properties, chemical specificities, low cost, easy processing, and scalable productions. Therefore, these nanomaterials have attracted much attention across a broad range of scientific and engineering disciplines. The transporting properties of conducting polymer nanowires have been studied in the context of two-terminal devices[1−6,8] and three-terminal devices,[7,9] including solid-state transistors and electrochemical transistors of thin conducting polymer films. The measurements of charge transport in conducting polymers bridged between two nanoelectrodes have been demonstrated by controlling the polymer redox states electrochemically.[10] Most recently, measurement of conductance of a thiol-terminated heptaaniline oligomer attached to gold electrodes in electrolyte solution has also been reported.[11] A three-terminal transistor[12,13] composed of drain, source, and gate electrodes provides an excellent platform for in-depth investigations of gating and doping effects, the nature of the doping, and the field-induced modulation (on/off current ratio) of conducting materials. In this device context, carbon nanotubes[14−18] and metal- and oxide-based nanowires[19−21] have been studied on electrochemical transistor platforms and subsequently harnessed for applications in nanoscale devices.

We have recently developed a template-free, site-specific electrochemical method to precise fabrication of an individually addressable conducting polymer (e.g., polyaniline) nanowires on electrode junctions (CPNEJs) in a parallel-oriented array.[5] These polymer nanowires, which formed a numerous intercrossing networks between the two electrodes with a gap of 2 μm, have uniform diameters ranging from 50 to 200 nm. We have demonstrated the excellent performance of the two-terminal resistive sensor devices using CPNEJ arrays in terms of their high sensitivity and their fast response for the detection of HCl and NH_3 gases, ethanol vapor, and the pH of NaCl solutions.[5] Since electrolyte-gated transistors that can be composed by introducing a remote gate electrode into the surrounding electrolyte solutions[15,22] have been utilized widely for chemo-[23] and biosensing purposes[9,24] because the gate-induced modulation provides another dimension of information in addition to the transport ($I-V$) characteristics obtained by two-terminal devices, our interest is to investigate the electrolyte gating transistor behavior of the CPNEJ array-based devices. Moreover, gate-induced modulation can be applied for signal amplification to enhance the detection performance of resistive sensors.[23,24] Thus, it is of great interest to explore the electrolyte-gated transistors based on CPNEJs.

In this paper, we report the properties of electrolyte-gated transistors based on conducting polymer nanowire electrode junctions (CPNEJs) that we fabricated upon lithographically patterned electrodes by using template-free electrochemical polymerization[1] at a low and constant current.[5,6] Three types of CPNEJs based on polyaniline, polypyrrole, and poly(ethylenedioxythiophene) (poly(EDOT)) were investigated. Our goals are to understand (i) the feasibility of electrolyte-gated transistors based on conducting polymer materials, i.e., polyaniline, polypyrrole, and poly(EDOT) nanowires, (ii) the doping nature of these conducting polymer nanowires and the gate-modulation effects on the currents (on/off ratios) of their corresponding electrolyte-gated transistors, and (iii) the influence that pH has on the doping nature of the conducting polymer nanowires as well as the on/off ratio of their transistors. In parallel, we have also investigated blank devices and electrolyte-gated transistors based on the conducting polymer thin films that serve as controls.

Experimental Section

The redox-active monomer precursors such as aniline, pyrrole, and ethylenedioxythiophene (EDOT) were purchased from Aldrich and were used after purification by distillation. The detailed fabrication of the individually addressable CPNEJs upon the electrode patterns where two sets (10 pairs) of junction electrodes are separated by 10 2-μm-wide gaps was described

* Author to whom correspondence should be addressed. Phone: (+1) 310-794-1977. Fax: (+1) 310-206-8975. E-mail: hrtseng@mednet.ucla.edu.

10.1021/jp050903k CCC: $30.25
Published on Web 06/11/2005

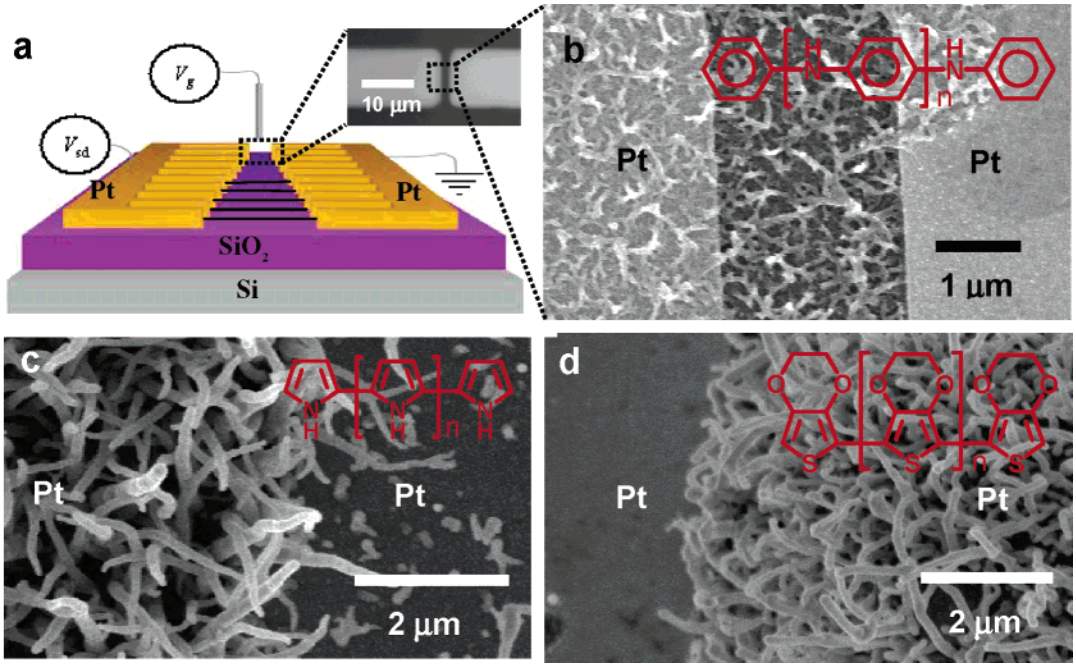

Figure 1. (a) Three-dimensional graphical representation of an electrolyte-gated transistor, in which 10 pairs of Pt electrodes serve as the source and drain. Conducting polymer nanowires were grown in the 10 2-μm-wide source−drain channels as the transport materials, and a suspended Pt wire functions as a gate electrode. Inset shows a 2-μm-wide source−drain channel. Scanning electron microscopy images and chemical structures of (b) polyaniline nanowires (ca. 40−80 nm in diameter), (c) polypyrrole nanowires (ca. 60−120 nm in diameter), and (d) poly(EDOT) nanowires (ca. 80−150 nm in diameter), which were grown electrochemically in the 10 2-μm-wide source−drain channels.

elsewhere.[5] These Pt electrodes (width, 10 μm; thickness, ca. 30 nm of Pt on 5 nm of Ti) were fabricated by standard photolithographic techniques and using electron beam deposition on a silicon (100) substrate covered with 500 nm of thermal oxide.[5] The conducting polymer nanowires including polyaniline, polypyrrole, or poly(EDOT) were introduced into the 10 2-μm-wide gaps by the template-free electrochemical polymerizations from their respective solutions in MilliQ/Millipore water containing aniline, pyrrole, or EDOT. The set of 10 electrodes was connected internally to a millimeter-scale electrode pad designated for attachment of wires. Before the fabrication of the CPNEJs, the electrode patterns were immersed in piranha solution (70% concentrated H_2SO_4/30% H_2O_2) for 2 min, rinsed with water, and then dried under a stream of N_2. The two sets of electrodes were then wire-bonded individually for connection to a potentiostat (Princeton 263A) and to the measurement systems. We performed the electrochemical production of the CPNEJs using an aqueous solution containing 0.2 M monomer precursor (pyrrole or EDOT) and 0.1 M $LiClO_4$ as the supporting electrolyte. We connected a standard three-port electrochemical configuration composed of working, counter, and reference electrodes to one set of junction electrodes, a Pt coil, and an Ag/AgCl reference electrode, respectively; the other set of electrodes remained unconnected. The electrochemical process that we employed for the production of the polymer nanowires within the 2-μm gaps can be divided into three continuous steps. In the first step, a constant current (50 nA) was applied for ca. 30 min to introduce the polymer nuclei onto the Pt working junction electrodes. Under this relatively high current, the effective potential on the working electrodes remains at ca. 0.68−0.58 V (vs the Ag/AgCl reference electrode). It is essential to produce these initial electrode-based polymer nuclei because they serve as seeds for the growth of the nanowires during the following two steps.

We characterized the morphology of the electrochemically fabricated polyaniline, polypyrrole, and poly(EDOT) nanowires by using a field emission scanning electron microscope (SEM; Hitachi S4700). The preparations of the electrolyte-gated transistors can be completed simply by immersing the CPNEJs (consisting of 10 pairs of drain and source electrodes) along with a gate electrode (a Pt wire or Ag/AgCl electrode) into a gate medium, i.e., buffered electrolyte solutions of NaCl with concentrations of 1.0, 0.1, and 0.01 M. The buffered electrolyte solutions of NaCl were prepared as follows: Appropriate amounts of NaCl were added to HCl solutions (for electrolyte solutions with pH values from 0 ± 0.1 to 4 ± 0.1), water (for pH values from 5 ± 0.1 to 9 ± 0.1), and NaOH solutions (for pH values from 0 ± 0.1 to 14 ± 0.1) respectively, and the resulting solutions were titrated to achieve the defined pH values by diluting the HCl and NaOH solutions in the presence of a pH meter.

A three-dimensional graphical representation (Figure 1a) illustrates the general configuration of these electrolyte-gated transistors, which are composed of a suspended Pt gate electrode, 10 parallel-oriented CPNEJs (one set of electrodes serves as the drain and the other set serves as the source), and the surrounding aqueous medium. However, the control devices incorporating thin films of polyaniline (Aldrich; M_w, 65 000; thickness, ca. 50 nm; spin-coated from its 0.2 wt % tetrahydrofuran solution), polypyrrole, and poly(EDOT) (thickness, ca. 90−120 nm; deposited by cyclic voltammetry (CV) in the water/acetonitrile (9:1 v/v) solutions containing pyrrole or EDOT) were also fabricated. The characterization of the electrolyte-gated transistors based on polymer nanowires in buffered aqueous media of NaCl at room temperature under ambient conditions were performed by using a semiconductor analyzer (Keithley 4200). The transistors were characterized with a gate potential sweep rate of 0.1 V/s and a drain−source voltage sweep rate of 0.01 V/s. The area of the Pt wire gate electrode exposed to the electrolyte solution is ca. 0.01 cm^2 as estimated from its diameter of 0.03 cm and the immerging length of 1.0 cm in the electrolyte solution. In the case of polymer nanowire

surface area, honestly, it is beyond the scope of our experiments to calculate the exact number of polymer nanowires and their surface areas because they form a network as can be seen in Figures 1b−d. In this study, both the drain and gate voltages (V_{sd} and V_g) were confined within the range from −0.8 to +0.8 V to eliminate the electrochemical influence associated with the aqueous media.

Results and Discussion

Figures 1b−d show the SEM images of polyaniline nanowires (ca. 50−80 nm in diameter), polypyrrole nanowires (60−120 nm in diameter), and poly(EDOT) nanowires (80−150 nm in diameter) in their respective CPNEJs. Immediately after their electrochemical fabrications, the polyaniline, polypyrrole, and poly(EDOT)-based CPNEJs exhibit resistances within the range of 300−2000 Ω.[5,6]

The drain current (I_{sd}) versus drain voltage (V_{sd}) characteristics of a polyaniline nanowire-based transistors obtained as a function of different positive gate voltages (V_g) are shown in Figure 2a. Unlike a solid-state transistor,[25,26] the value of I_{sd} rises upon increasing positive V_g at a negative V_{sd}. In fact, this phenomenon is consistent with the prior measurements performed on polyaniline-based break junctions[7a] and thin-film[7c] devices. It is important to note that the value of I_{sd} of the nanowire-based transistors was observed as high as 670 μA at $V_g = 0.8$ V and $V_{sd} = -0.8$ V; as a control, a maximum leakage current of 0.24 μA was observed for the blank devices under otherwise identical measurement conditions (Figure 2b). However, no saturation behavior of the $I_{sd}-V_{sd}$ curves was observed, which is due to the confinement of low drain and gate voltages (−0.8 to +0.8 V) as well as the potential contribution of ionic conduction.[7d] The observed leakage current (i.e., gate current (I_g)) of the nanowire-based transistor was in the same range of the blank devices (Figure 2c). These observations suggest that the leakage current is smaller than I_{sd} by a factor of 2800; it is totally negligible when it is taken into account with the value of I_{sd}. In addition, we performed an experiment in the way that the Pt wire electrode was connected as the drain instead of the gate, and the polymer nanowire-based CPNEJs were connected to the source and gate electrodes while keeping the other conditions constant to rule out the electrochemical effects associated with the electrodes. In fact, very low output current (I_{sd}) in the range 80−150 nA with no current modulation was observed even at the high gate voltage (0.8 or −0.8 V) and high V_{sd} (0.8 or −0.8 V). These experiments clearly suggest that the gated modulation observed in Figure 2a should be attributed to the polyaniline nanowires between the drain−source electrodes.

We calculated the resulting on/off current ratio of the Pt-wire-immersed electrolyte-gated polyaniline nanowire-based transistor from the drain currents (I_{sd}) at $V_g = 0.8$ V and $V_g = 0$ V (Figure 2a) to be 978. Within experimental error, this on/off current ratio is highly reproducible without any decrease upon repeatedly operating five transistors. Under similar conditions, but applying a negative V_g, we observed a very weak gate modulation for the nanowire-based transistors (Figure 3a), which indicates that the n-channel transport mechanism does not function in these transistors in aqueous media at pH 7 ± 0.1. Figure 3b displays a plot of $|I_{sd}|$ versus V_g at a constant drain voltage (a representative value of $V_{sd} = -0.5$ V) for the polyaniline nanowire-based transistor derived from Figures 2a and 3a. We observed a reversible hysteresis (forward I_{sd} (black curve) and reverse I_{sd} (red curve)) of the transistor in the V_g ranging from −0.8 to +0.8 V. For other values of V_{sd}, very

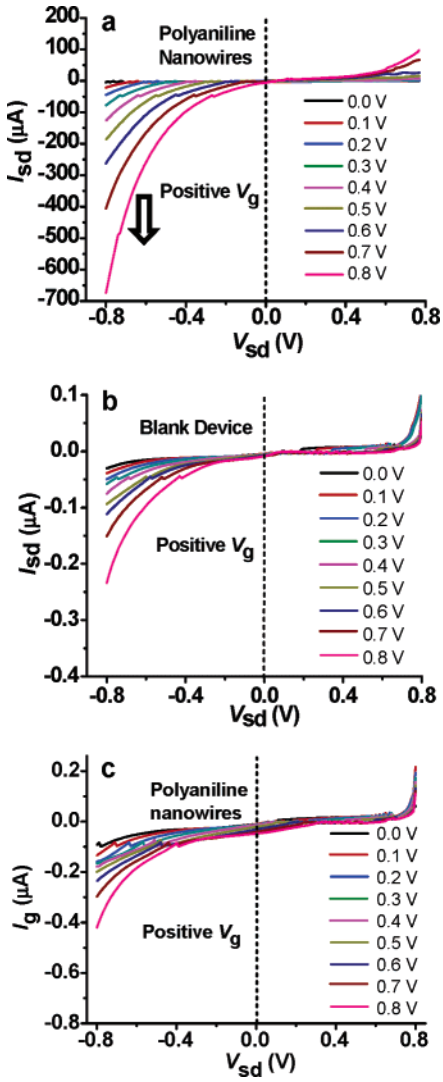

Figure 2. Drain current (I_{sd}) versus drain voltage (V_{sd}) characteristics of (a) an electrolyte-gated transistor based on polyaniline nanowires under positive gate biases ($V_g = 0$ to 0.8 V; step = 0.1 V; gate voltage sweep rate = 0.1 V/s) and (b) a blank device in a buffered aqueous medium containing 1.0 M NaCl at pH 7 ± 0.1. (c) Gate current (I_g) versus drain voltage (V_{sd}) characteristics of the same electrolyte-gated transistor based on polyaniline nanowires under positive gate biases ($V_g = 0$ to 0.8 V; step = 0.1 V; gate voltage sweep rate = 0.1 V/s) in 1.0 M NaCl electrolyte solution at pH 7 ± 0.1.

similar hysteresis curves were observed. It can be concluded that polyaniline nanowires are excellent p-type materials[25,26] and that polyaniline nanowire-based transistors have large gate-induced modulation, i.e., on/off current ratio. We characterized the control transistors based on 50-nm polyaniline thin films under identical conditions. The maximum on/off current ratio was 156, which is a factor of 6 smaller than that of the nanowire-based transistors.

To understand the role of the ionic strength of the NaCl electrolyte solutions and their influence on the current modulation of the polymer nanowire-based transistors, we characterized four devices (two for polyaniline-based CPNEJs and two for polypyrrole-based CPNEJs) in different concentrations (1.0, 0.1, and 0.01 M) of the NaCl electrolyte solutions while keeping the other experimental conditions and the geometry identical. The values of I_{sd} of the polyaniline nanowire-based transistors increase upon increasing the gate voltage (V_g) at a negative V_{sd} in both 0.1 and 0.01 M NaCl electrolyte solutions as shown in Figures 4a and 4b, respectively. The observed shape and charac-

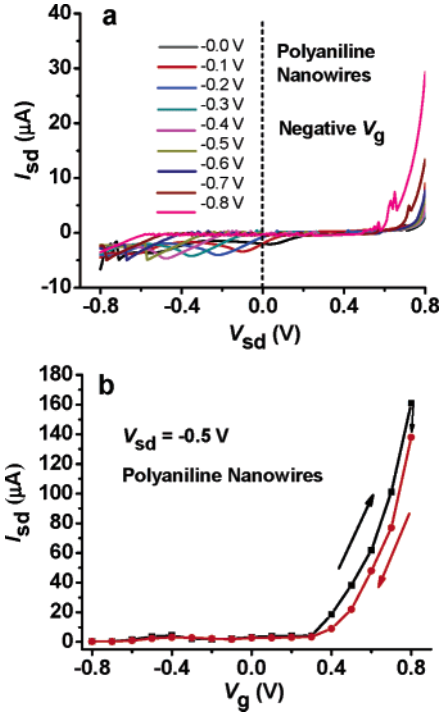

Figure 3. (a) $I_{sd}-V_{sd}$ characteristics of a polyaniline nanowire-based transistor under negative gate biases ($V_g = 0$ to -0.8 V; step = 0.1 V; gate voltage sweep rate = 0.1 V/s) under otherwise identical measurement conditions as those in Figure 2. (b) Plot of $|I_{sd}|$ versus gate voltage (V_g) for the polyaniline nanowire-based transistor at a constant V_{sd} (-0.5 V). This $I_{sd}-V_g$ plot is derived from the $I_{sd}-V_{sd}$ characteristics presented in Figures 2a and 3a.

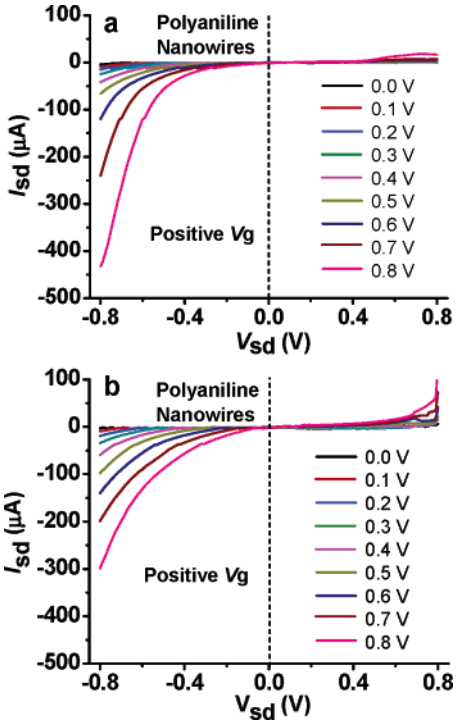

Figure 4. Drain current (I_{sd}) versus drain voltage (V_{sd}) characteristics of an electrolyte-gated transistor based on polyaniline nanowires under positive gate biases ($V_g = 0$ to 0.8 V; step = 0.1 V; gate voltage sweep rate = 0.1 V/s) in (a) 0.1 M NaCl electrolyte solution and (b) 0.01 M NaCl electrolyte solution at pH 7 ± 0.1.

teristics of the $I_{sd}-V_{sd}$ curves of the transistors in both the 0.1 and the 0.01 M NaCl electrolyte solutions are identical to that in 1.0 M NaCl solutions. The maximum values of I_{sd} of the

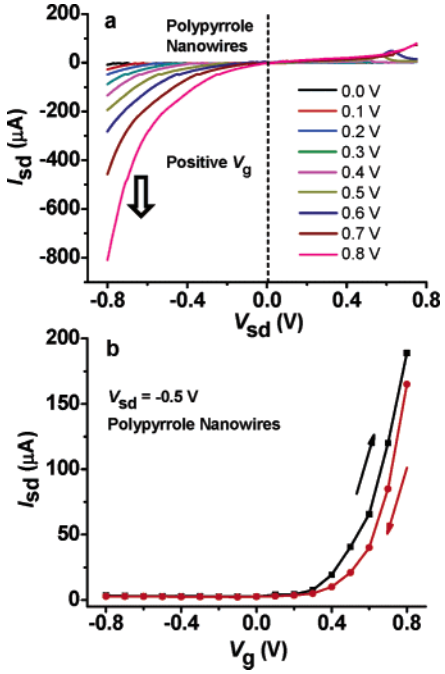

Figure 5. (a) $I_{sd}-V_{sd}$ characteristics of electrolyte-gated transistors based on polypyrrole nanowires under positive gate biases ($V_g = 0$ to 0.8 V; step = 0.1 V; gate voltage sweep rate = 0.1 V/s) in a buffered aqueous medium containing 1.0 M NaCl at pH 7 ± 0.1. (b) Plot of $|I_{sd}|$ versus gate voltage (V_g) for the polypyrrole nanowire-based transistor at a constant V_{sd} (-0.5 V). This $I_{sd}-V_g$ plot is derived from the $I_{sd}-V_{sd}$ characteristics presented in part a.

transistors were 425 and 298 μA in the 0.01 M NaCl solutions, respectively, at $V_g = 0.8$ and $V_{sd} = -0.8$ V, which are relatively lower than that observed in 1.0 M NaCl electrolyte solution, while the on/off current ratios (610−690) are similar for all of the devices. These results clearly show that the decreases of I_{sd} are not proportional to the change of concentrations (10−100 dilution) of the NaCl electrolyte solutions used in this study, suggesting that the observed current modulation by applied gate voltages is mainly due to the modulation of carrier density in the polymer nanowires although a minor ionic carrier contribution is always operating and cannot be ruled out. As a control, the maximum leakage currents obtained for the blank devices were decreased proportionally with the decreasing concentrations of the NaCl electrolyte solutions (Supporting Information).

We then characterized the electrolyte-gated transistors based on polypyrrole nanowires (60−120 in diameter) in a buffered (pH 7.0 ± 0.1) aqueous medium of 1.0 M NaCl at room temperature under ambient conditions. Figure 5a shows the characteristic $I_{sd}-V_{sd}$ curves of polypyrrole nanowire-based transistors in which I_{sd} rises upon increasing positive V_g at a negative V_{sd}, indicating that holes are the major charge carriers (p-type) in the polypyrrole nanowires as in the polyaniline nanowires described above. The value of I_{sd} was observed as high as 810 μA at $V_g = 0.8$ V and $V_{sd} = -0.8$ V, which is a factor of 3375 larger than the leakage current observed for the blank devices. Therefore, the leakage current can be neglected again. The on/off current ratio of the device obtained from the I_{sd} at $V_g = 0.8$ V and $V_g = 0$ V is 175, which is also reproducible within the experimental error upon repeatedly operating seven transistors. The $|I_{sd}|-V_g$ curves obtained at a constant drain voltage ($V_{sd} = -0.5$ V) for the polypyrrole nanowire-based transistor show a reversible hysteresis (forward I_{sd} (black curve) and reverse I_{sd} (red curve); Figure 5b). Similar to polyaniline nanowire-based devices, no n-channel transistor characteristics

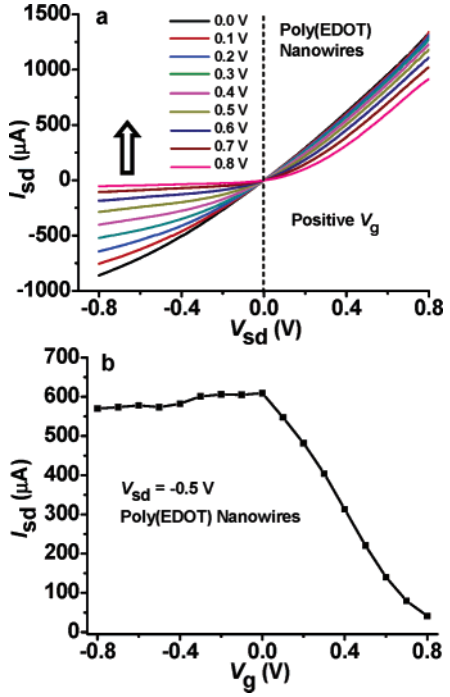

Figure 6. (a) $I_{sd}-V_{sd}$ characteristics of electrolyte-gated transistors based on poly(EDOT) nanowires under positive gate biases ($V_g = 0$ to 0.8 V; step = 0.1 V; gate voltage sweep rate = 0.1 V/s) in a buffered aqueous medium containing 1.0 M NaCl at pH 7 ± 0.1. (b) Plot of $|I_{sd}|$ versus gate voltage (V_g) for the poly(EDOT) nanowire-based transistor at a constant V_{sd} (−0.5 V). This $I_{sd}-V_g$ plot is derived from the $I_{sd}-V_{sd}$ characteristics presented in part a.

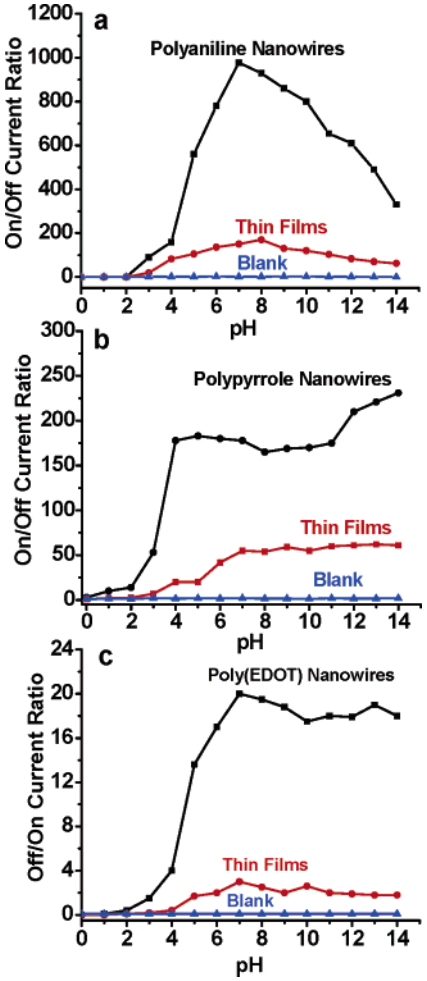

Figure 7. Plots of the pH-dependent on/off current ratios of (a) polyaniline and (b) polypyrrole and off/on current ratios of (c) poly(EDOT) nanowire-based transistors. The control experiments based on the respective polymer thin-film (red) and blank (blue) devices are also presented. These data were acquired under a positive V_g in aqueous 1.0 M NaCl media at different values of pH (from 0 ± 0.1 to 14 ± 0.1).

were observed at negative V_g for the polypyrrole nanowire-based transistors under an identical characterization condition. Additionally, a control transistor based on electrochemically deposited polypyrrole thin films (ca. 100 nm) was studied to give a maximum on/off current ratio of 55.

In contrast to polyaniline and polypyrrole nanowire-based transistors, poly(EDOT) nanowire-based transistors exhibit opposite behavior under the similar characterization conditions. Both the $I_{sd}-V_{sd}$ and the $|I_{sd}|-V_g$ curves (Figures 6a and 6b) showed that the values of I_{sd} of poly(EDOT) nanowire-based transistors decrease upon increasing positive V_g at a negative V_{sd}, which indicates that depletion-mode p-channel transistor characteristics are functioning in poly(EDOT) nanowires.[7d,27−30] For the poly(EDOT) nanowire-based transistors, the observed off current was as high as 860 μA at $V_g = 0.0$ V and $V_{sd} = -0.8$ V, the on current was as low as 40 μA at $V_g = 0.8$ V and $V_{sd} = -0.8$ V, and the resulting off/on current ratio was calculated to be ca. 20, which is highly reproducible within the experimental error upon repeatedly operating three transistors. Once again, no n-channel transistor characteristics were observed at negative V_g for the poly(EDOT) nanowire-based transistors, and a control transistor based on poly(EDOT) thin films (ca. 110 nm) was studied to give a maximum off/on current ratio around 4.

It is well-known that some conducting polymer nanowires, e.g., polyaniline and polypyrrole, can be doped and dedoped by the actions of acid and base, respectively, which leads to dramatic changes in their transporting properties.[31,32] We were interested in determining the relationship between the doped/dedoped transport properties and the field-induced modulation in the transistor. We investigated the polyaniline, polypyrrole, and poly(EDOT) nanowire-based transistors in aqueous media at different values of pH (ranging from 0 to 14). It is crucial to note here that the aqueous media contain 0.01, 0.1, and 1.0 M NaCl to adjust the ionic strength and ensure that similar background conductances are experienced by all of the transistors in the aqueous media. At the same time, we employed blank devices lacking either polymer nanowires or thin films in the 2-μm-wide drain−source channel as controls to monitor the background signals and the leakage current. As the results indicate, we observed the maximum leakage current within the range from 0.05 to 0.2 μA in aqueous media at pH 4−14; these values of leakage current are negligible when compared with the values of I_{sd} observed for the polymer nanowire- and thin-film-based transistors.

For the polyaniline nanowire-based transistors, in the aqueous media having values of pH in the range from 0 to 14, we observed a positive-V_g-induced modulation of I_{sd} upon performing a negative sweep of V_{sd} from 0.0 to −0.8 V. No transistor behavior was observed at pH 3 or below. We observed similar trends in the on/off current ratios for the control transistors but with lower magnitudes in the field-induced properties. Figure 7a summarizes the results that we observed for the polyaniline nanowire-based transistors and the control devices (thin-film-based transistors and blank devices). The transistor characteristics in response to the values of the pH of the gate media can be divided into three distinct regimes: (1) a highly doped conductor regime (pH 0−3 ± 0.1) in which no transistor

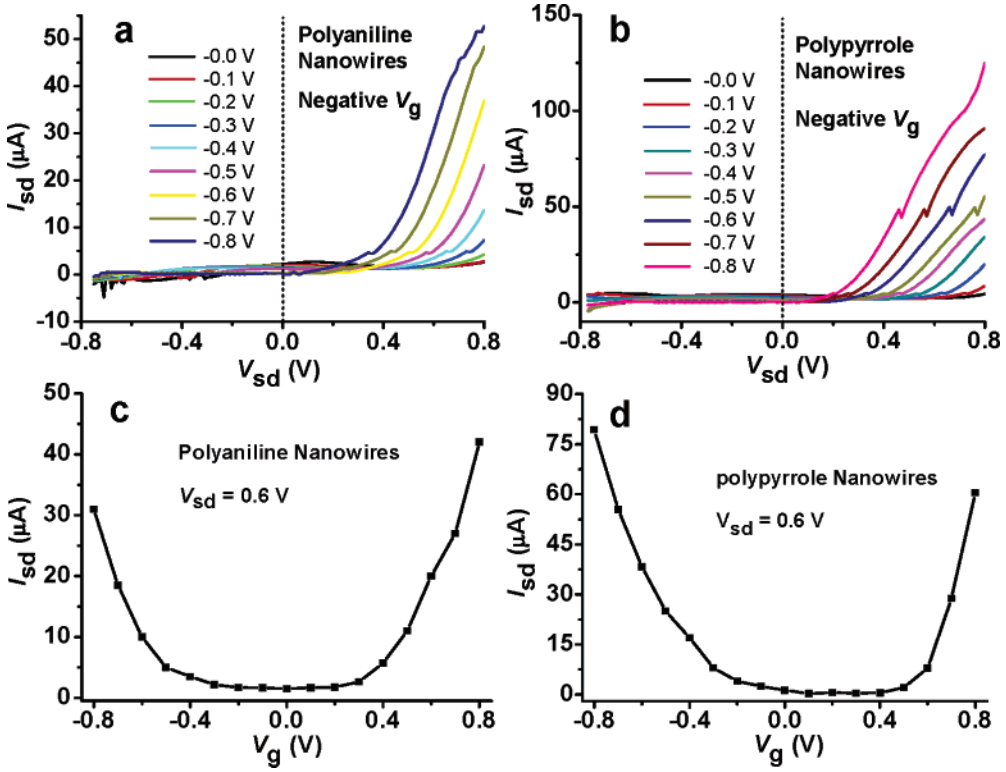

Figure 8. $I_{sd}-V_{sd}$ characteristics of electrolyte-gated transistors based on (a) polyaniline and (b) polypyrrole nanowires under negative gate biases (V_g = 0 to −0.8 V; step = 0.1 V; gate voltage sweep rate = 0.1 V/s) in a buffered aqueous medium containing 1.0 M NaCl at pH 11 ± 0.1. Plot of $I_{sd}-V_g$ at a constant positive drain voltage (V_{sd} = 0.6 V) for (c) the polyaniline and (d) the polypyrrole nanowire-based transistors in the same buffer solutions.

properties were observed because the highly doped polyaniline exhibits an ohmic (metallic) behavior, (2) a partially doped semiconductor region (pH 4−7 ± 0.1)[31] in which the transistor on/off current ratios increase upon increasing the value of the pH, and (3) a partially dedoped semiconductor regime (pH > 7 ± 0.1) in which the on/off current ratios decrease upon increasing the value of the pH. Since polyaniline shows multiple oxidation (doping) states,[31,32] which are dependent on the pH of the surrounding environment, it could be the reason that we observed three distinct regions of on/off ratios for polyaniline transistors at different pH values. In addition, we want to point out that the on/off current ratios of the polyaniline nanowire-based transistors are 5−7-fold better than those of the polyaniline thin-film-based transistors at all values of the pH. The better on/off ratios of polyaniline nanowires can be attributed to large surface-area-to-volume ratio of the nanowires compared to that of the films. In the cases of polypyrrole and poly(EDOT) nanowire-based transistors (Figures 7b and 7c), in a conductor (metallic) regime (pH 0−3), no transistor properties were observed. At pH region 4−6 ± 0.1, the on/off current ratios increase upon increasing the pH value. When the pH value is larger than 4, the on/off current ratios reach a plateau of 170−250 for polypyrrole nanowire-based transistors (Figure 7b). Unlike transistors based on polyaniline and polypyrrole nanowires that contain acid/base-sensitive N−H groups, no significant change in the off/on ratio (ca. 15−20) was observed for the poly(EDOT) nanowire-based transistors in the media with pH values ranging from 4 ± 0.1 to 14 ± 0.1 (Figure 7c). Just like polyaniline nanowire-based transistors, the on/off and off/on current ratios of the polypyrrole and poly(EDOT) nanowire-based transistors are 5−6-fold better than those of their corresponding thin-film-based transistors at all values of the pH.

In the acidic conditions (pH 0 to 4 ± 0.1), we did not observe transistor properties (Figure 7), which may due to nonreversible redox processes and also due to the highly doped metallic behavior of the polymers. We have further operated the transistors with the drain−source voltage (V_{sd}) in the range from −0.6 to +0.6 V (Supporting Information) to rule out the nonreversible electrochemical contribution. In fact, we observed similar transistor behaviors in terms of both $I-V$ characteristics and on/off current ratios in the pH range from 6 ± 0.1 to 14 ± 0.1, whereas no transistor performance was observed in the acidic media (pH 0−4 ± 0.1). These results suggest that the transistor behavior observed for the devices in the pH range 6 ± 0.1 to 14 ± 0.1 is due to carrier density modulation in the polymer nanowires through applied gate voltage to the devices. However, the nonreversible electrochemical redox processes may occur in acidic media at pH <5.

The polymer nanowire-based transistors were also characterized by using an Ag/AgCl electrode as a gate electrode at different pH values (5, 7, 9, 11, and 13) of the NaCl electrolyte solutions. We observed similar $I_{sd}-V_{sd}$ characteristic curves with a maximum I_{sd} of 500 μA at V_g = 0.8 and V_{sd} = −0.8 V, which is a factor of 1.4−2.4 smaller than that observed using Pt wire as the gate electrode (Figures 2a and 5a). The calculated on/off current ratios were in the range 110−355 for polyaniline nanowire-based transistors and 100−125 for polypyrrole nanowire-based transistors. In both these cases, we found lower device performance, which may be due to the use of the Ag/AgCl electrode as a gate electrode in the transistor geometry. From the $I_{sd}-V_g$ plots for both polyaniline and polypyrrole nanowire-based transistors (Supporting Information), we found only a slight change in the threshold gate voltages; no significant change in the threshold gate voltages was observed even using the Ag/AgCl as a gate electrode.

In the basic gate media (pH > 9), we observed a negative gate-modulated transistor behavior for both the polyaniline and polypyrrole nanowire-based transistors (Figures 8a and 8b).

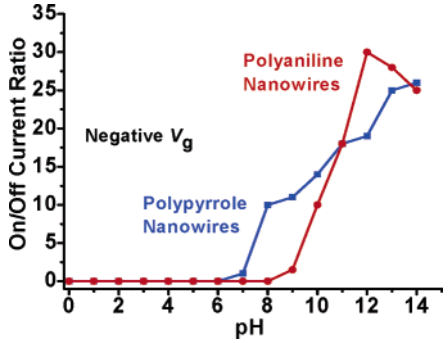

Figure 9. Plots of the pH-dependent on/off current ratios of polyaniline (red) and polypyrrole (blue) nanowire-based transistors. We acquired these data under a negative V_g in aqueous media containing 1.0 M NaCl at different values of pH (from 0 ± 0.1 to 14 ± 0.1).

When polyaniline-based transistors were measured at $V_g = -0.8$ V and $V_{sd} = 0.8$ V, the values of I_{sd} were obtained in the range of 40−70 μA; these values are a factor of 10−15-fold smaller than those observed for the positive gated modulations. In the case of polypyrrole nanowire-based transistors, the values of I_{sd} were in the range of 100−125 μA at $V_g = -0.8$ V and $V_{sd} = 0.8$V and a factor of 6−8-fold smaller than those observed for the positive gated modulations. The plots of $I_{sd}-V_g$ at a constant positive drain voltage ($V_{sd} = 0.6$ V) for both the polyaniline and the polypyrrole nanowire-based transistors measured at pH 11 ± 0.1 are shown in Figures 8c and 8d, respectively. The $I_{sd}-V_g$ traces clearly show the increase of I_{sd}, i.e., an increase in the conductivity of the polyaniline and the polypyrrole nanowires under both negative gate modulation (e.g., threshold negative V_g ca. −0.3 V for polyaniline and ca. −0.1 V for polypyrrole) and positive gate modulation (e.g., threshold positive V_g ca. 0.2 V for polyaniline and ca. 0.4 V for polypyrrole). Similar $I_{sd}-V_g$ traces were observed for polyaniline and polypyrrole nanowire-based transistors in the basic media (pH 9−14 ± 0.1). These observations suggest that an increase in conductivity under the negative gate modulation is due to electron conduction, whereas hole conduction is responsible under the positive gate modulation at higher pH values (>9). The observed on/off current ratios are 5−30 for both the polyaniline and the polypyrrole nanowire-based transistors with the negative gate modulation in basic media (pH > 9; Figure 9). These results suggest that the polyaniline and polypyrrole nanowires can act as n-type semiconducting materials in basic media, but negative gate modulation effects in the polyaniline and polypyrrole nanowire-based transistors are less significant than the positive gate modulation. Under similar measurement conditions, no negative gate-modulated transistor behavior was observed for poly(EDOT) nanowires.

Conclusions

We have demonstrated electrolyte-gated polyaniline, polypyrrole, and poly(EDOT) nanowire-based transistors using electrochemically fabricated CPNEJs in the NaCl aqueous media at different values of pH (1−14). We observed p-channel transistor characteristics of the polymer nanowires at pH 7, including a large on/off current ratio of ca. 1×10^3 for polyaniline nanowire-based transistors. Similarly, the polypyrrole-based CPNEJs also show p-channel transistor behaviors, whereas the poly(EDOT)-based CPNEJs exhibit depletion-mode behaviors. Because an ideal biosensor must function in neutral biological solutions, e.g., phosphate-buffered saline (PBS) solution, the polyaniline and polypyrrole nanowire-based transistors that we report herein are perfectly suitable for biological sensing applications. According to our approach, a conducting polymer nanowire-based two-terminal resistive device can be converted into a three-terminal transistor by simply immersing the device into an electrolyte solution along with a gate electrode. In these cases, the field-induced modulation can be applied for signal amplification to enhance the performance; in addition, it can provide another dimension of information along with the transport ($I-V$) characteristic obtained in the two-terminal device context. Our long-term objective is to introduce the advantages provided by the gate electrode into a sensor array that incorporates a variety of individually addressable conducting polymer nanoframeworks to realize the ultrasensitive, real-time, parallel detection of analytes in solution.

Acknowledgment. This research was supported in the David Geffen School of Medicine at UCLA by the Crump Institute for Molecular Imaging, by the Department of Molecular and Medical Pharmacology, and by the Developmental Award from the UCLA Prostate SPORE. We thank Professor James R. Heath, Dr. Yi Luo, and Dr. Guanglu Ge at Caltech Chemistry for their help during electrode fabrication.

Supporting Information Available: $I_{sd}-V_{sd}$ characteristics of polypyrrole nanowire-based transistors under positive gate biases, $I_{sd}-V_{sd}$ characteristics of blank devices, $I_{sd}-V_{sd}$ characteristics of nanowire-based transistors with a drain−source voltage sweep range from 0.6 to +0.6 V, $|I_{sd}|$ versus V_g for the polyaniline nanowire-based transistors, and $|I_{sd}|$ versus V_g for the polypyrrole nanowire-based transistors. This material is available free of charge via the Internet at http://pubs.acs.org.

References and Notes

(1) Liang, L.; Liu, J.; Windisch, C. F.; Exarhos, G. J.; Lin, Y. H. *Angew. Chem., Int. Ed.* **2002**, *41*, 3665.
(2) Huang, J. X.; Virji, S.; Weiller, B. H.; Kaner, R. B. *J. Am. Chem. Soc.* **2003**, *125*, 314.
(3) Hatano, T.; Bae, A. H.; Takeuchi, M.; Fujita, N.; Kaneko, K.; Ihara, H.; Takafuji, M.; Shinkai, S. *Angew. Chem., Int. Ed.* **2004**, *43*, 465.
(4) Ramanathan, K.; Bangar, M. A.; Yun, M. H.; Chen, W. F.; Mulchandani, A.; Myung, N. V. *Nano Lett.* **2004**, *4*, 1237.
(5) Wang, J.; Chan, S.; Carlson, R. R.; Luo, Y.; Ge, G.; Ries, R. S.; Heath, J. R.; Tseng, H.-R. *Nano Lett.* **2004**, *4*, 1693.
(6) Wang, J.; Alam, M. M.; Guo, Y.; Tseng, H.-R., submitted for publication.
(7) (a) He, H. X.; Li, C. Z.; Tao, N. J. *Appl. Phys. Lett.* **2001**, *78*, 811. (b) Merlo, J. A.; Frisbie, C. D. *J. Polym. Sci., Part B: Polym. Phys.* **2003**, *41*, 2674. (c) Paul, E. W.; Ricco, A. J.; Wrighton, M. S. *J. Phys. Chem.* **1985**, *89*, 1441. (d) Nilsson, D.; Chen, M.; Kugler, T.; Remonen, T.; Armgarth, M.; Berggren, M. *Adv. Mater.* **2002**, *14*, 51.
(8) Liu, H. Q.; Kameoka, J.; Czaplewski, D. A.; Craighead, H. G. *Nano Lett.* **2004**, *4*, 671.
(9) Bartlett, P. N.; Astier, Y. *Chem. Commun.* **2000**, 105.
(10) (a) He, H. X.; Li, X. L.; Tao, N. J.; Nagahara, L. A.; Amlani, I.; Tsui, R. *Phys. Rev. B* **2003**, *68*, 045302. (b) He, H. X.; Zhu, J. S.; Tao, N. J.; Nagahara, L. A.; Amlani, I.; Tsui, R. *J. Am. Chem. Soc.* **2001**, *123*, 7730.
(11) Chen, F.; He, J.; Nuckolls, C.; Roberts, T.; Klare, J. E.; Lindsay, S. *Nano Lett.* **2005**, *5*, 503.
(12) Katz, H. E.; Bao, Z. N.; Gilat, S. L. *Acc. Chem. Res.* **2001**, *34*, 359.
(13) Horowitz, G. *Adv. Mater.* **1998**, *10*, 365.
(14) Tans, S. J.; Verschueren, A. R. M.; Dekker, C. *Nature* **1998**, *393*, 49.
(15) Rosenblatt, S.; Yaish, Y.; Park, J.; Gore, J.; Sazonova, V.; McEuen, P. L. *Nano Lett.* **2002**, *2*, 869.
(16) Bradley, K.; Cumings, J.; Star, A.; Gabriel, J.-C. P.; Gruner, G. *Nano Lett.* **2003**, *3*, 639.
(17) Siddons, G. P.; Merchin, D.; Back, J. H.; Jeong, J. K.; Shim, M. *Nano Lett.* **2004**, *4*, 927.
(18) Star, A.; Gabriel, J.-C. P.; Bradley, K.; Gruner, G. *Nano Lett.* **2003**, *3*, 459.
(19) Zhong, Z. H.; Wang, D. L.; Cui, Y.; Bockrath, M. W.; Lieber, C. M. *Science* **2003**, *302*, 1377.

(20) Wang, D. W.; Wang, Q.; Javey, A.; Tu, R.; Dai, H. J.; Kim, H.; McIntyre, P. C.; Krishnamohan, T.; Saraswat, K. C. *Appl. Phys. Lett.* **2003**, *83*, 2432.
(21) Xia, Y. N.; Yang, P. D. *Adv. Mater.* **2003**, *15*, 351.
(22) Kruger, M.; Buitelaar, M. R.; Nussbaumer, T.; Schonenberger, C.; Forro, L. *Appl. Phys. Lett.* **2001**, *78*, 1291.
(23) Bradley, K.; Gabriel, J.-C. P.; Briman, M.; Star, A.; Gruner, G. *Phys. Rev. Lett.* **2003**, *91*, 218301.
(24) Bradley, K.; Briman, M.; Star, A.; Gruner, G. *Nano Lett.* **2004**, *4*, 253.
(25) Kuo, C. T.; Chiou, W. H. *Synth. Met.* **1997**, *88*, 23.
(26) (a) Kuo, C. T.; Chen, S. A.; Hwang, G. W.; Kuo, H. H. *Synth. Met.* **1998**, *93*, 155. (b) White, H. S.; Kittlesen, G. P.; Wrighton, M. S. *J. Am. Chem. Soc.* **1984**, *106*, 5375.
(27) Zhu, Z.-T.; Mabeck, J. T.; Zhu, C.; Cady, N. C.; Batt, C. A.; Malliaras, G. G. *Chem. Commun.* **2004**, 1556.
(28) (a) Epstein, A. J.; Hsu, F.-C.; Chiou, N.-R.; Prigodin, V. N. *Curr. Appl. Phys.* **2002**, *2* 339. (b) Lu, J.; Pinto, N. J.; MacDiarmid, A. G. *J. Appl. Phys.* **2002**, *92*, 6033.
(29) Nilsson, D.; Kugler, T.; Svensson, P.-O.; Berggren, M. *Sens. Actuators B* **2002**, *86*, 193.
(30) Pinto, N. J., Jr.; Johnson, A. T.; MacDiarmid, A. G.; Mueller, C. H.; Theofylaktos, N.; Robinson, D. C.; Miranda, F. A. *Appl. Phys. Lett.* **2003**, *83*, 4244.
(31) Macdiarmid, A. G.; Chiang, J. C.; Richter, A. F.; Epstein, A. J. *Synth. Met.* **1987**, *18*, 285.
(32) Polk, B. J.; Potje-Kamloth, K.; Josowicz, M.; Janata, J. *J. Phys. Chem. B* **2002**, *106*, 11457.